Open Access on 08/18/2015

ARTICLE

NanoScript: A Nanoparticle-Based Artificial Transcription Factor for Effective Gene Regulation

Sahishnu Patel,[†,⊥] Dongju Jung,[‡,⊥] Perry T. Yin,[§] Peter Carlton,[‡] Makoto Yamamoto,[∥] Toshikazu Bando,[∥] Hiroshi Sugiyama,[‡,∥] and Ki-Bum Lee[†,§,*]

[†]Department of Chemistry and Chemical Biology, Rutgers, The State University of New Jersey, Piscataway, New Jersey 08854, United States, [‡]Institute for Integrated Cell-Material Sciences (iCeMS), Kyoto University, Kyoto, Japan, [§]Department of Biomedical Engineering, Rutgers, The State University of New Jersey, Piscataway, New Jersey 08854, United States, and [∥]Department of Chemistry, Graduate School of Science, Kyoto University, Kyoto, Japan. [⊥]S. Patel and D. Jung contributed equally.

ABSTRACT Transcription factor (TF) proteins are master regulators of transcriptional activity and gene expression. TF-based gene regulation is a promising approach for many biological applications; however, several limitations hinder the full potential of TFs. Herein, we developed an artificial, nanoparticle-based transcription factor, termed NanoScript, which is designed to mimic the structure and function of TFs. NanoScript was constructed by tethering functional peptides and small molecules called synthetic transcription factors, which mimic the individual TF domains, onto gold nanoparticles. We demonstrate that NanoScript localizes within the nucleus and initiates transcription of a reporter plasmid by over 15-fold. Moreover, NanoScript can effectively transcribe targeted genes on endogenous DNA in a nonviral manner. Because NanoScript is a functional replica of TF proteins and a tunable gene-regulating platform, it has great potential for various stem cell applications.

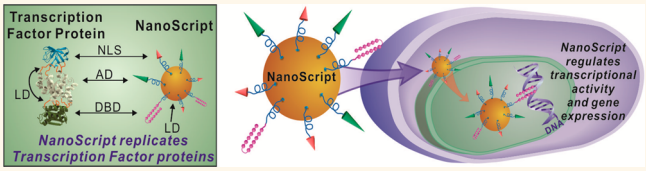

KEYWORDS: nanoparticle-based genetic manipulation · transcription factor proteins · gene activation · synthetic transcription factors · nonviral delivery

Gene regulation by ectopic expression of key transcription factors (TFs) not only has high impact in the field of biomedical research but also attracts significant research insight in terms of regulating gene expression.[1] By initiating complex signaling cascades and manipulating genetic circuitry, TFs regulate fundamental cellular behaviors and can also override cellular identity to reprogram and differentiate cells into specific lineages.[2] TFs are master regulators of gene expression and are structurally composed of multiple domains, of which three essential domains are (i) a nuclear localization signal (NLS) domain to shuttle TFs into the nucleus, (ii) a DNA-binding domain (DBD), which binds to predefined DNA sequences in the promoter region of target genes, and (iii) an activation domain (AD), which recruits the transcriptional machinery complex to the binding site to initiate transcription.

Protein therapy, which involves delivering proteins into cells to replace dysfunctional proteins, holds immense potential for applications focusing on regulating gene expression and cellular behaviors such as cellular reprogramming, cancer treatment, and stem cell therapy.[3] Numerous approaches including electroporation, nanocapsules, lipid micelles, polymer-based carriers, and nanoparticle-based delivery have been developed for intracellular protein delivery.[4−9] However, practical application of these methods for gene-regulating applications is limited because proteins, especially TFs, that are exogenously introduced into the cells have low delivery efficiency, cannot regulate genetic pathways at the transcriptional level, lack cell-specific targeting capabilities, and, above all, are extremely vulnerable to degradation by intracellular proteases.[10,11]

Rather than designing just another protein delivery vehicle, we sought to develop an innovative platform that replicates the fundamental function of TF proteins using a nanomaterial-based small-molecule approach. Nanomaterials, such as gold nanoparticles (AuNPs), have desirable physiochemical as well as nanostructural properties and have

* Address correspondence to kblee@rutgers.edu.

Received for review March 21, 2014 and accepted August 18, 2014.

Published online August 18, 2014
10.1021/nn501589f

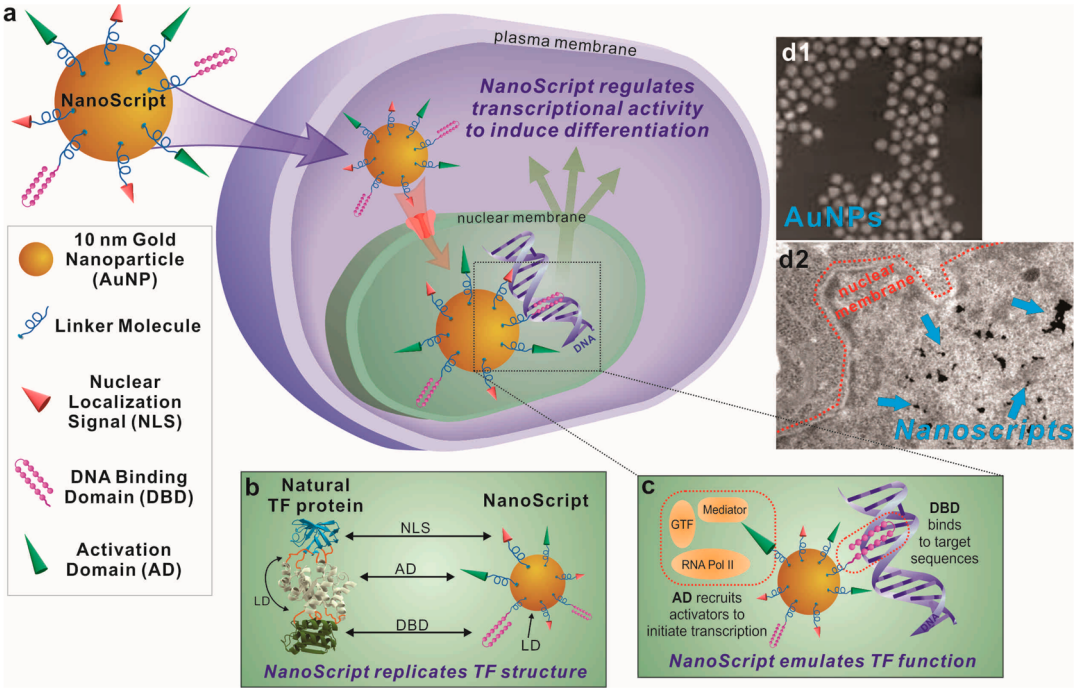

Figure 1. Schematic representation of NanoScript's design and function. (a) By assembling individual STF molecules, including the DBD, AD, and NLS, onto a single 10 nm gold nanoparticle, we have developed the NanoScript platform to replicate the structure and function of TFs. This NanoScript penetrates the cell membrane and enters the nucleus through the nuclear receptor with the help of the NLS peptide. Once in the nucleus, NanoScript interacts with DNA to initiate transcriptional activity and induce gene expression. (b) When comparing the structure of NanoScript to representative TF proteins, the three essential domains are effectively replicated. The linker domain (LD) fuses the multidomain protein together and is replicated by the AuNP. (c) The DBD binds to complementary DNA sequences, while the AD recruits transcriptional machinery components such as RNA polymerase II (RNA Pol II), mediator complex, and general transcription factors (GTFs). The synergistic function of the DBD and AD moieties on NanoScript initiates transcriptional activity and expression of targeted genes. (d) The AuNPs are monodisperse and uniform. The NanoScript constructs are shown to effectively localize within the nucleus, which is important because transcriptional activity occurs only in the nucleus.

been successfully established for biological applications.[12,13] Along with these unique attributes, the biological inertness and high stability in physiological conditions make AuNPs excellent carriers of small molecules and biomolecules.[14] Recently, chemical biologists developed a class of small molecules, called synthetic transcription factors (STFs), that have been demonstrated to mimic the function of each TF domain, albeit with limited success.[15−20]

Herein, we demonstrate development of a novel nanoparticle-based artificial transcription factor, termed NanoScript, which replicates the multidomain structure and gene-regulating function of natural TFs (Figure 1a). NanoScript replicates the multidomain structure of TF proteins because the three major components, which represent the three major domains (NLS, DBD, and AD) found on endogenous TFs, are tethered together in close proximity on a single AuNP (Figure 1b). In addition to serving as a delivery vehicle for STFs, the AuNP itself serves as a functional component of the NanoScript because it mimics the linker domain (LD) of natural TF proteins (Figure 1b). NanoScript emulates the gene-regulating function of TFs because the three STF components, which include (i) a NLS peptide, (ii) a hairpin polyamide DBD, and (iii) a transactivation peptide AD, all function synergistically to regulate transcriptional activity of targeted genes in a nonviral manner (Figure 1c).

The NanoScript platform presented here has several advantageous features such as a multifunctional AuNP surface that allows attachment of all STF components with a flexible density onto a single nanoparticle, a compact hydrodynamic size (<42 nm diameter) for effective nuclear localization and DNA intercalation with intrinsic multivalent interactions, an ability to target selective predetermined genes, a nonintegrative mechanism for regulating genes, and an inert AuNP core for maximal stability and biocompatibility under physiological conditions (Figure 1d). As a result, our carefully designed NanoScript can localize within the nucleus and effectively initiate transcriptional activity of both a reporter plasmid and endogenous genes. It is important to note that NanoScript does not deliver TF proteins but, instead, acts as a functional platform that is designed to behave like them.

RESULTS AND DISCUSSION

Construction and Characterization of NanoScript. NanoScript was synthesized by assembling three essential components on AuNPs. The first is a hairpin polyamide

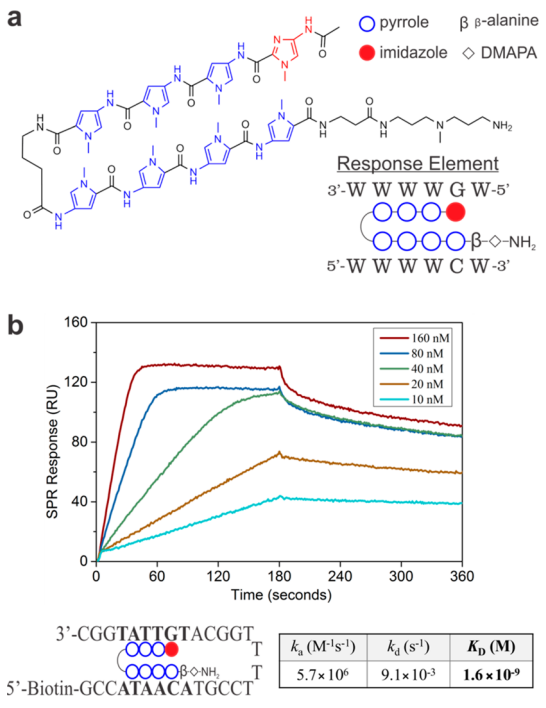

k_a ($M^{-1}s^{-1}$)	k_d (s^{-1})	K_D (M)
5.7×10^6	9.1×10^{-3}	1.6×10^{-9}

Figure 2. The Py-Im hairpin polyamide has high binding affinity for the target sequence. (a) The hairpin polyamide structures of the DBD containing pyrrole (Py) and imidazole (Im) motifs, which bind to A-T and G-C base pairs, respectively, are arranged to target the 3′-WWWWGW-5′ sequence (W = A or T). The hairpin polyamide DBD is anchored with a dimethylaminopropylamine (DMAPA) moiety to enable conjugation. (b) SPR sensorgrams show the interaction of varying polyamide DBD concentrations with complementary hairpin DNAs. The equilibrium constant (K_D), which is indicative of the binding affinity, was determined by the ratio of the dissociation constant (k_d) to the association constant (k_a).

structure (representing the DBD), which was specifically chosen because of its high specificity to target DNA sequences and exceptionally high binding affinity that is comparable to naturally occurring DNA-binding proteins.[21,22] The hairpin polyamide is composed of *N*-methylpyrrole (Py) and *N*-methylimidazole (Im) amino acids, which bind to complementary A-T and G-C motifs on the DNA, respectively.[23] Using solid-phase synthesis, a polyamide was synthesized with amino acids arranged in the order ImPyPyPy-γ-PyPyPyPy-β-Dp-NH_2 (γ is γ-aminobutyric acid, β is β-alanine, and Dp is dimethylaminopropylamide), to recognize the 5′-WGWWWW-3′ (W = A or T) DNA sequence (Figure 2a). This sequence was specifically chosen to recognize the matching DNA sequence of our proof-of-concept reporter plasmid, which will be used to evaluate its gene-regulating functionality (details described below). Using surface plasmon resonance, the binding affinity of the polyamide to its target sequence was determined to have a remarkably high nanomolar affinity with an equilibrium constant of 1.6×10^{-9} M (Figure 2b). In addition, the polyamide binding affinity to a mismatched DNA sequence decreased by over 70-fold, thus implying the polyamide is specific for its target sequence (Figure S1).

The second component (representing the AD) is a synthetic transactivation peptide that was synthesized in the D-form to resist intracellular degradation and is capable of activating transcriptional activity by recruiting mediators, RNA polymerase II, SAGA, and other proteins to the binding site.[24−26] The third component (representing the NLS domain) is a nuclear localization signal peptide derived from the SV40 large T-antigen and functions to shuttle NanoScript into the nucleus.[27−29]

These three components were then assembled onto a single nanoparticle using a carefully designed conjugation chemistry to develop NanoScript. The NanoScript platform was constructed by first coating AuNPs with mercaptoundeconic acid (MUA) and then conjugating the three STF components *via* EDC/NHS coupling (Figure 3a). This reaction was carried out in a controlled buffered (pH = 6.0−7.4) solution to ensure conjugation through the primary amine, but there is a possibility that NLS binds either directly to the AuNP or through lysine side chains, which should not influence its functionality.[29] Adsorption of the STF components on the AuNPs was confirmed by UV spectroscopy, which indicated a successive shift of the surface plasmon peak (Figure S2). On the basis of previous reports, we are confident the DBD conjugated to NanoScript binds preferentially to the target sequence.[30] In terms of the STF ratio on NanoScript, we speculated a high ratio of NLS would be required because translocation of NanoScript into the nucleus is one of the most critical barriers for effective gene activation. Furthermore, we anticipated that a minimal ratio of the polyamide DBD would be required because of its exceptionally high binding affinity to DNA and that the ratio of AD be doubled in order to mimic the potent endogenous TF p53.[31] Therefore, we designed NanoScript to have an optimum ratio of STF components and quantified the surface ratio using high-pressure liquid chromatography (HPLC) analysis (Table S1).

The physical properties were characterized using dynamic light scattering, which determined the hydrodynamic diameter of NanoScript to be 34.0 ± 2.3 nm and the surface charge to be −32.5 mV (Figure 3b). This hydrodynamic diameter is in excellent agreement with the theoretical value, because, based on calculating bond lengths, we predicted the theoretical diameter of NanoScript to be 35.2 nm. Electron micrographs of NanoScript confirmed that surface functionalization with STF components did not affect the size distribution or monodispersity of the nanoparticles (Figure 3c). The stability of both NanoScript and MUA-coated AuNPs (Au-MUA) was tested in various physiological environments including water, PBS, and culture media and showed that the nanoparticles remained stable in these environments, as indicated by minimal shifts in the absorbance peak (Figure S3).

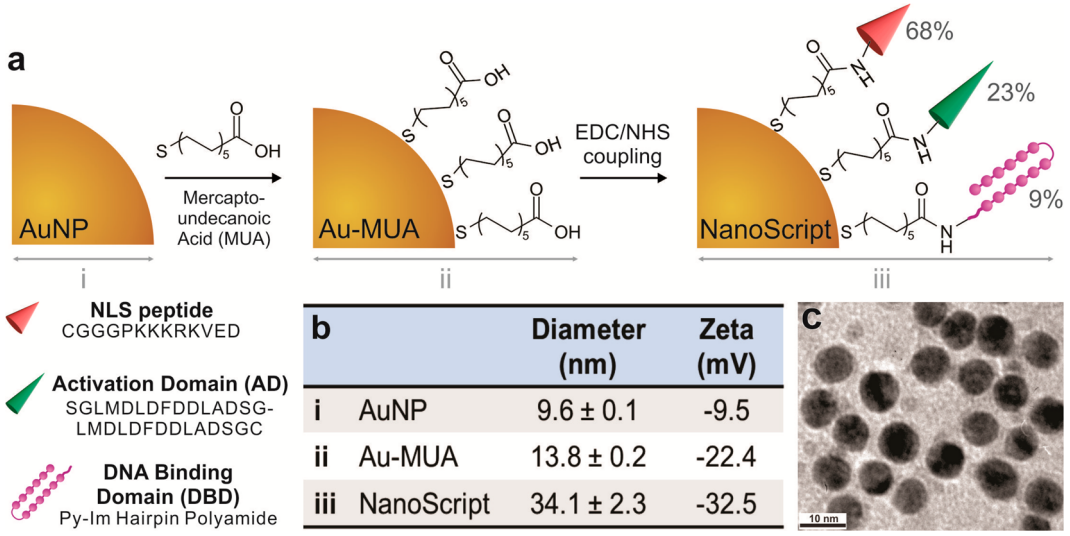

Figure 3. Construction and characterization of NanoScript. (a) AuNPs of 10 nm are first coated with mercaptoundecanoic acid (MUA), then activated with EDC/NHS coupling chemistry, and finally the small-molecule components are assembled to construct NanoScript. This reaction was carried out in a controlled buffered (pH = 6.0−7.4) solution to ensure conjugation through the primary amine, but there is a possibility that NLS binds either directly to the AuNP or through lysine side chains, which should not influence its functionality. (b) The hydrodynamic diameter of NanoScript increases stepwise with the conjugation of functional components. The surface charge of NanoScript also increases stepwise with the addition of more negatively charged components. (c) TEM micrograph showing a monodisperse and uniform distribution of NanoScript.

Nuclear Localization of NanoScript. Efficient nuclear localization of NanoScript is especially important because transcriptional activity occurs exclusively in the nucleus. To this end, NanoScript was specifically designed with a small hydrodynamic diameter (~34.0 nm as mentioned above) because the nuclear pore, which tightly regulates cargo transport across the nuclear envelope, has a maximum diameter of approximately 44 nm.[32−34] The plasma membrane permeability of NanoScript was assessed by first incubating NanoScript with HeLa cells for 4 h and then quantifying the number of particles that were able to enter the cells using inductively coupled plasma atomic emission spectroscopy (ICP-OES). Analysis revealed that NanoScript was able to efficiently penetrate the plasma membrane in just 4 h of incubation, as compared to the control (NanoScript without NLS peptide), which showed minimal uptake (Figure 4a), which indicates that the NLS peptide also plays a significant role in enabling NanoScript to enter the cell. To monitor intracellular localization, NanoScript was labeled with a fluorescent dye and incubated in HeLa cell cultures. Fluorescence images, taken with a 3D structured illumination microscope, shows that NanoScript is able to target and penetrate the nuclear envelope (Figure 4b, Figure S4). As indicated by the phase contrast image, the HeLa cells seem to remain intact (Figure S5). Additionally, a side-view image indicates that NanoScript is evenly dispersed throughout the nucleus in the vertical plane, thus confirming that NanoScript is not merely resting on the surface of the nucleus (Figure 4c). Furthermore, a three-dimensional fluorescence video shows NanoScript distributed throughout the nucleus, thereby providing further confirmation of nuclear uptake (Video S1).

Given the potential for degradation of NanoScript components by intracellular proteases, we wanted to ensure that the observed fluorescence overlap was not due to components being cleaved from NanoScript and diffusing into the nucleus, but rather that the nanoparticles were able to enter the nucleus intact. For this purpose, we performed TEM on cellular cross sections to determine if intact NanoScript was able to enter the nucleus. The TEM image shows the interface between the cytoplasm and the nucleus, with NanoScript clearly located inside the nucleus (Figure 4d, Figure S6). While this indicates that the NLS peptide may be initially conjugated on NanoScript, there is high probability that cytoplasmic proteases degrade the NLS peptide over a longer period of time. Combining the results of the fluorescence and TEM images, NanoScript was demonstrated to effectively enter the nucleus while remaining intact, which would be critical for achieving high transcriptional activity.

Transcriptional Activation Using NanoScript. The primary function of TFs is to regulate transcriptional activity; hence we evaluated NanoScript's ability to control transcription and gene expression. As a proof-of-concept experiment, we constructed a reporter plasmid containing a response element with *six tandem copies* of the 5′-TGTTAT-3′ sequence, which is selectively recognized by the polyamide DBD molecule (Figure 5a).[17] This response element is located 36 base pairs upstream from the TATA box to facilitate initiation of transcriptional activity (Figure S7). Transcription of this

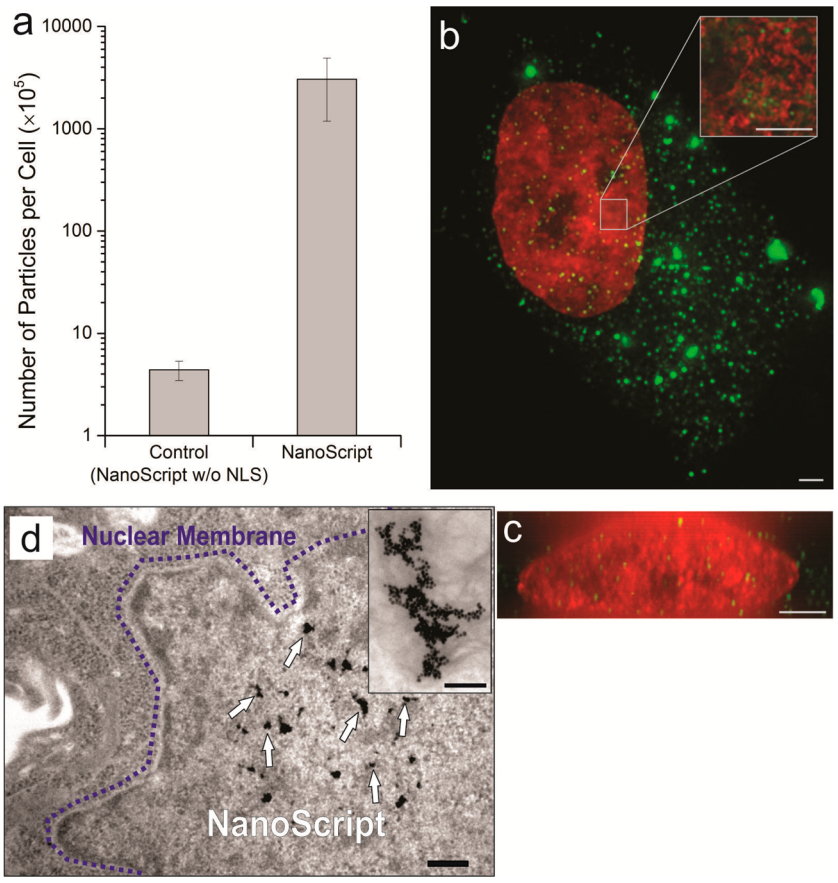

Figure 4. NanoScript effectively localizes within the nucleus. (a) HeLa cells were first incubated with NanoScript for 4 h, and the number of particles that penetrated the plasma membrane and entered the HeLa cells was quantified thereafter. After 48 h, (b) a fluorescence image showed NanoScript (green) scattered throughout the cell and inside the nucleus (red), (c) and a side view of the nucleus (red) reveals that NanoScript (green) is evenly dispersed throughout the nucleus (scale bar = 2 μm). (d) A TEM micrograph of a nuclear cross-section shows NanoScript clusters (black dots) localized within the nucleus (scale bar = 200 nm). A magnified image of NanoScript clusters (inset) shows individual nanoparticles (scale bar = 100 nm).

reporter plasmid produces alkaline phosphatase (ALP), which can be quantified using a colorimetric assay. Since the secreted ALP is directly proportional to the magnitude of induced transcriptional activity, the functionality and potency of NanoScript can be evaluated and quantified. After cotransfecting NanoScript and the reporter plasmid into HeLa cells, ALP levels were measured after 48 h (Figure 5b). Analysis revealed that NanoScript induces transcription and overexpresses the reporter plasmid by 15-fold in comparison to unmodified AuNPs (Figure 5c), while maintaining high cell viability (Figure S8). Furthermore, the contribution of each component on NanoScript for initiating transcriptional activity was tested by selectively removing each component. Subsequent ALP analysis of control experiments showed limited gene expression, thus confirming the importance and synergistic activity of each STF component on NanoScript (Figure 5c). A positive control included transfecting the same concentrations of DBD and AD molecules as on the nanoparticle to the culture media and showed a 2.2-fold increase in gene transcription, a result that is similar to the previously reported studies. Moreover, when cells were exposed to varying NanoScript concentrations, there was dose-dependent transcriptional activation (Figure 5d).

NanoScript Activates Endogenous Genes. In order to fully emulate the gene-regulating function of TFs and to establish the NanoScript platform suitable for potential biological applications, it is essential that NanoScript can activate endogenous genes on native DNA. For this purpose, several genes including *LGALS8* and *EGLN3* were identified to contain numerous response elements that complement the polyamide DBD (Table S2).[17] The number of complementary binding sites on endogenous DNA is not expected to be directly proportional to the level of gene activation, primarily due to the nucleosome/histone packaging of DNA and variability in binding site availability.[35] Quantification of endogenous gene activation showed that the expression of *LGALS8* and *EGLN3* was increased 65% and 58%, respectively, relative to unmodified AuNPs (Figure 5e). Successful gene activation indicates that NanoScript can interact with endogenous DNA, seek complementary gene motifs, and initiate transcriptional activity of targeted endogenous genes. It is important to note

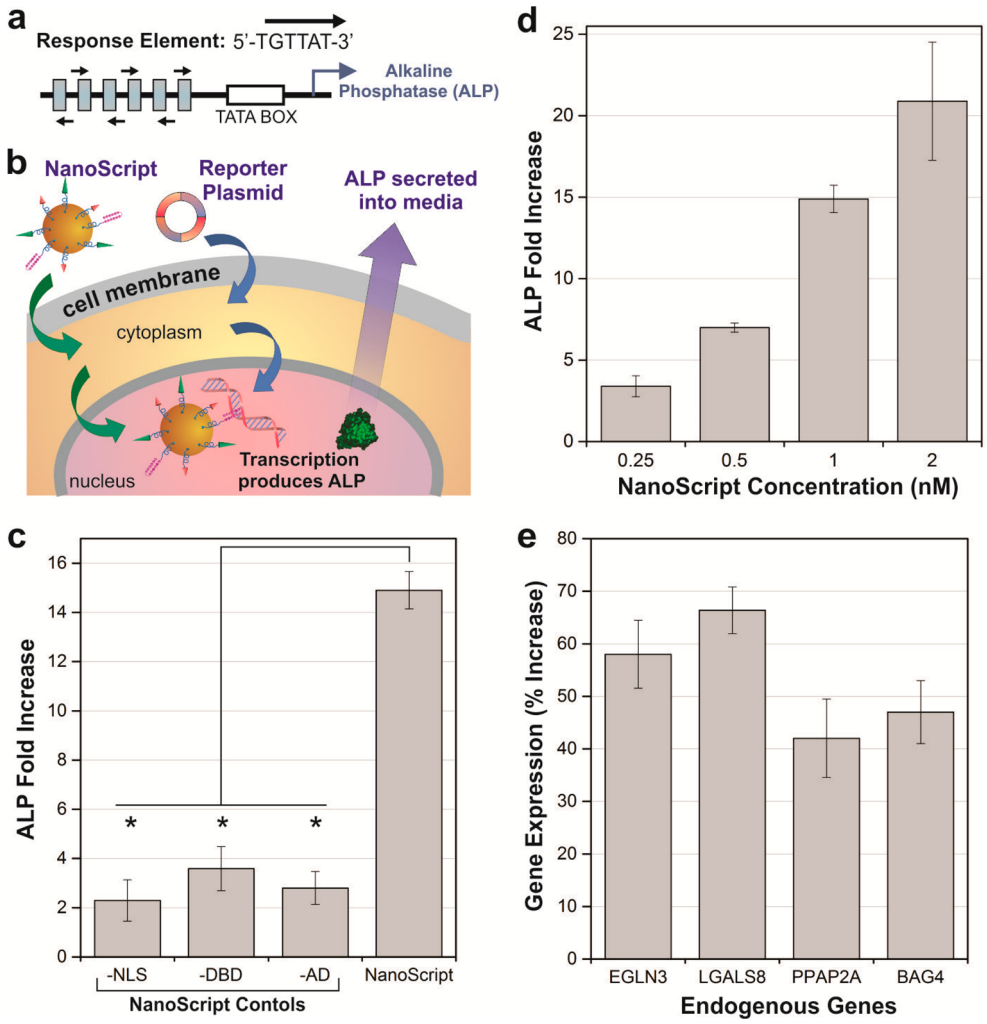

Figure 5. NanoScript transcribes a reporter plasmid and activates endogenous genes. (a) The reporter gene containing six copies of the response element is located upstream from the TATA box and secretes alkaline phosphatase (ALP) upon transcription. (b) Schematic representation of co-delivering the reporter plasmid and NanoScript. After NanoScript and the reporter plasmid both localize within the nucleus, transcriptional activity is initiated to produce ALP, which is secreted into the culture media. (c) ALP fold induction initiated by NanoScript (1 nM) compared to controls that lack individual components. (d) Concentration-dependent induction of ALP by NanoScript. (e) HeLa cells were incubated with NanoScript (1 nM), and 48 h later, qPCR analysis reveals activation of targeted genes. Standard error, mean, and *t* test analysis for all experiments was derived from three individual trials. ALP was measured 48 h post-transfection, and fold increase is relative to unmodified AuNP controls.For *t* test analysis * indicates $p < 0.01$.

that the gene activation of the reporter plasmid was expected to be higher than the activation of endogenous genes because endogenous genes are tightly coiled into nucleosomes while reporter plasmids are not, thus making the reporter plasmid more prone to being transcribed. The overexpression of endogenous genes highlights the versatility and functionality of NanoScript, thus proving that this platform can behave and function like natural TFs.

CONCLUSIONS

Most previously reported methods to regulate gene expression involve either viral vectors (*e.g.*, DNA plasmids and retroviruses),[36,37] small molecules (*e.g.*, RNAi and synthetic molecules) that regulate translation or target a specific signaling pathway,[38−40] or nanomaterial-based exogenous cues (*e.g.*, nanotopographical surface patterns).[40−44] However, NanoScript is the first nanomaterial-based platform that mimics natural TFs and interacts with endogenous DNA to regulate gene expression at the transcriptional level in a nonviral manner.

Several remarkable features of NanoScript enable translation of this platform for applications that require gene manipulation. First, because gene expression by NanoScript is nonviral, this platform is an attractive alternative to conventional viral-based methods for regulating forced gene activation. Second, the multifunctional AuNP surface of NanoScript can potentially allow for attachment of additional moieties such as histone modification molecules, cell-specific targeting peptides, and RNAi molecules for an enhanced and synergistic regulation of gene expression.[45−47] Third, the AuNP backbone of NanoScript can be replaced

with other types of nanoparticles, such as upconverting nanoparticles and magnetic core−shell nanoparticles, for potential applications such as tracking gene regulation in real time through infrared imaging or magnetic resonance imaging (MRI), respectively.[43,48] Finally, the most advantageous feature of NanoScript is its tunable components, by simply redesigning the hairpin polyamide DBD sequence to target regulatory genes such as those involved in differentiation. However, it should be noted that, due to the short DBD targeting sequence, there is a possibility for interactions with off-target genes; hence, further optimization by designing DBDs with longer sequences to target longer DNA sequences would further enhance the NanoScript platform. Overall, the NanoScript platform has great potential to be utilized for stem cell biology or reprogramming applications.

In summary, we have developed an innovative NanoScript platform, which effectively replicates the multidomain structure and gene-regulating function of naturally occurring TFs. As a proof-of-concept experiment, we show NanoScript to effectively regulate gene expression of both a reporter plasmid and endogenous genes on native DNA. Due to the unique tunable properties of NanoScript, we are highly confident this platform not only will serve as a desirable alternative to conventional gene-regulating methods but also has direct employment for applications involving gene manipulation such as stem cell differentiation, cancer therapy, and cellular reprogramming.

METHODS

Synthesis of Gold Nanoparticles. The gold nanoparticles with an approximate diameter of 9 nm were prepared by the Ferns method of citrate reduction of $HAuCl_4$ following establish protocols. All glassware was cleaned in aqua regia (3:1 HCl/HNO_3, *handle with extreme caution!*), then rinsed with nanopure water and oven-dried. A 50 mL aqueous solution of 1 mM $HAuCl_4$ was heated to reflux while stirring. Then 8 mL of 1% (by weight) sodium citrate was quickly added, resulting in a change in solution color from yellow to ruby red. After the color change, the solution was heated to reflux for another 5 min, then cooled to room temperature and filtered using a 0.45 μm syringe filter. Size distribution was characterized using transmission electron microscopy (TEM) and dynamic light scattering (DLS), and concentration was obtained using UV−vis spectroscopy.

Construction of NanoScript. Ten nanometer gold nanoparticles were conjugated to ligands using a two-step method. The first step involves ligand exchange on the AuNP with the linker molecule 11-mercaptoundecanoic acid. First, from a stock solution of MUA dissolved in ethanol, 1 mM MUA was added to the AuNP solution (pH = 11, NaOH) and allowed to stir at room temperature for 24 h. The solution was then filtered three times using a 10 000 MWCO filter (Millipore) and resuspended in distilled water. The second step involves conjugating the ligands to the AuNP *via* the carboxylic acid of the MUA. To the AuNP solution, adjusted to pH = 6.5 by adding 5 mM MES (Hampton Research), was added 0.3 mM 1-ethyl-3-(3-(dimethylamino)propyl)carbodiimide) (EDC) (Sigma) and 0.75 mM *N*-hydroxysuccinimide (NHS) (Acros Organics), and the resulting solution was allowed to stir for 2 h at room temperature. The solution was filtered three times using a 10K MWCOF and resuspended in 1 mM MES water. Immediately afterward, a solution containing a 10 M excess of NLS peptide, transactivation peptide (TAP), and hairpin-polyamide DBD with a mole ratio of 7:2:1 (NLS:TAP:DBD) was added dropwise to the AuNP solution, adjusted to pH = 7.2 by adding 50 mM HEPES (Cellgro) prior to addition of biomolecules, and allowed to stir for 2 h. The AuNP solution was filtered three times using a 10 000 MWCO to remove unreacted molecules.

The dye-labeled NanoScript, used for tracking intracellular localization, was constructed by modifying the AD (the transactivation peptide) with a fluorescent dye (Alexa Fluor 568 Hydrazide, Invitrogen). Specifically, the dye was conjugated to the transactivation peptide *via* EDC/NHS coupling as described above.

NanoScript Characterization. The NanoScript construct was characterized using multiple techniques. First, the concentration of the gold nanoparticles and confirmation of conjugation were found using UV−visible absorption spectra (Varian Cary 5000 UV−vis−NIR spectrophotometer). Second, DLS (Malvern Zetasizer Nano-ZS90) was utilized to measure the size and zeta potential (surface charge) of the AuNP construct after each conjugation step to find the hydrodynamic diameter and surface charge, respectively. Third, the morphology of the AuNP core was determined using TEM analysis. The AuNPs were drop-cast on the holey-carbon grids (Electron Microscopy Sciences), allowed to dry overnight under vacuum, and subsequently imaged using a JEOL JEM-2010F high-resolution TEM operated at an accelerating voltage of 200 kV. Finally, the amount of peptides on NanoScript's surface was calculated by performing HPLC (Agilent LC 1100) using a Zorbax Extend-C18 Solvent Saver Plus, 3.5 μm, 3.0 × 150 mm, column. The peptide solution before conjugation and the supernatant solution after conjugation, which contained unreacted peptides, were both analyzed using HPLC. The exact number of moles for each peptide was calculated using a standard curve comparing the concentration and area. The difference in moles for each peptide before and after conjugation was calculated. The ratio of the difference in moles is attributed to the ratio on the nanoparticle. For this experiment, after the nanoparticles were centrifuged at 12 000 rpm for 20 min, the supernatant was collected and analyzed.

HeLa Cell Culture and NanoScript Uptake. HeLa cells were cultured in Dulbecco's modified Eagle medium with high glucose (DMEM) (Invitrogen) supplemented with 10% fetal bovine serum, 1% Glutamax (Invitrogen), and 1% streptomycin−penicillin antibiotic in a 37 °C humidified incubator with 5% CO_2. Prior to transfection, 25 000 HeLa cells were seeded in a well of a 24-well plate. After 24 h, the cells were incubated with a mixture of the 1 nM NanoScript solution, 0.5 μg of the reporter plasmid, and X-tremeGENE (Roche) in Opti-MEM medium (Invitrogen). After 4 h, the cells were washed twice with PBS and fresh culture medium was added. After 48 h, the alkaline phosphatase level in the culture medium was tested using the SEAP chemiluminescence kit 2.0 (Clontech) following the manufacturer's protocol. An MTS assay (Promega) was also performed at this time to test cell viability.

Conflict of Interest: The authors declare no competing financial interest.

Acknowledgment. We are grateful to Valentine Starovoytov (Rutgers University) for his help in sample preparation and TEM imaging. We are grateful to Ganesh Pandian Namasivayam (Kyoto University) for performing SPR experiments. K.B.L. acknowledges financial support from the NIH Director's Innovator Award (1DP20D006462-01), the NIH R21 grant (1R21NS085569-01), the N.J. Commission on Spinal Cord grant (CSR13ERG005), and the Rutgers Faculty Research Grant Program.

Supporting Information Available: The Supporting Information files contain experimental details of STF synthesis, SPR binding affinity, cell TEM, reporter plasmid design, PCR analysis, ICP analysis, and immunocytochemistry. Figures and tables

include UV absorbance of NanoScript, ligand ratio on nanoparticle surface, TEM micrograph of NanoScript, reporter plasmid sequence, cell viability, and number of complementary binding sites on DNA. A Nuclear Localization 3D video is also available. This material is available free of charge *via* the Internet at http://pubs.acs.org.

REFERENCES AND NOTES

1. Reik, W. Stability and Flexibility of Epigenetic Gene Regulation in Mammalian Development. *Nature* **2007**, *447*, 425–432.
2. Spitz, F.; Furlong, E. E. M. Transcription Factors: From Enhancer Binding to Developmental Control. *Nat. Rev. Genet.* **2012**, *13*, 613–626.
3. Leader, B.; Baca, Q. J.; Golan, D. E. Protein Therapeutics: A Summary and Pharmacological Classification. *Nat. Rev. Drug Discovery* **2008**, *7*, 21–39.
4. Liu, Y.; Wang, H.; Kamei, K.-i.; Yan, M.; Chen, K.-J.; Yuan, Q.; Shi, L.; Lu, Y.; Tseng, H.-R. Delivery of Intact Transcription Factor by Using Self-Assembled Supramolecular Nanoparticles. *Angew. Chem., Int. Ed.* **2011**, *50*, 3058–3062.
5. Yan, M.; Du, J.; Gu, Z.; Liang, M.; Hu, Y.; Zhang, W.; Priceman, S.; Wu, L.; Zhou, Z. H.; Liu, Z.; *et al*. A Novel Intracellular Protein Delivery Platform Based on Single-Protein Nanocapsules. *Nat. Nanotechnol.* **2010**, *5*, 48–53.
6. Choi, S.-O.; Kim, Y.-C.; Lee, J. W.; Park, J.-H.; Prausnitz, M. R.; Allen, M. G. Intracellular Protein Delivery and Gene Transfection by Electroporation Using a Microneedle Electrode Array. *Small* **2012**, *8*, 1081–1091.
7. Tang, R.; Kim, C. S.; Solfiell, D. J.; Rana, S.; Mout, R.; Velázquez-Delgado, E. M.; Chompoosor, A.; Jeong, Y.; Yan, B.; Zhu, Z.-J.; *et al*. Direct Delivery of Functional Proteins and Enzymes to the Cytosol Using Nanoparticle-Stabilized Nanocapsules. *ACS Nano* **2013**, *7*, 6667–6673.
8. Gu, Z.; Biswas, A.; Zhao, M.; Tang, Y. Tailoring Nanocarriers for Intracellular Protein Delivery. *Chem. Soc. Rev.* **2011**, *40*, 3638–3655.
9. Bale, S. S.; Kwon, S. J.; Shah, D. A.; Banerjee, A.; Dordick, J. S.; Kane, R. S. Nanoparticle-Mediated Cytoplasmic Delivery of Proteins To Target Cellular Machinery. *ACS Nano* **2010**, *4*, 1493–1500.
10. Carter, P. J. Introduction to Current and Future Protein Therapeutics: A Protein Engineering Perspective. *Exp. Cell Res.* **2011**, *317*, 1261–1269.
11. Dimitrov, D. Therapeutic Proteins. In *Therapeutic Proteins*; Voynov, V.; Caravella, J. A., Eds.; Humana Press, 2012; Vol. 899, pp 1–26.
12. Rosi, N. L.; Giljohann, D. A.; Thaxton, C. S.; Lytton-Jean, A. K. R.; Han, M. S.; Mirkin, C. A. Oligonucleotide-Modified Gold Nanoparticles for Intracellular Gene Regulation. *Science* **2006**, *312*, 1027–1030.
13. Wang, Z.; Liu, H.; Yang, S. H.; Wang, T.; Liu, C.; Cao, Y. C. Nanoparticle-Based Artificial RNA Silencing Machinery for Antiviral Therapy. *Proc. Natl. Acad. Sci. U.S.A.* **2012**, *109*, 12387–12392.
14. Giljohann, D. A.; Seferos, D. S.; Daniel, W. L.; Massich, M. D.; Patel, P. C.; Mirkin, C. A. Gold Nanoparticles for Biology and Medicine. *Angew. Chem., Int. Ed.* **2010**, *49*, 3280–3294.
15. Mapp, A. K.; Ansari, A. Z.; Ptashne, M.; Dervan, P. B. Activation of Gene Expression by Small Molecule Transcription Factors. *Proc. Natl. Acad. Sci. U.S.A.* **2000**, *97*, 3930–3935.
16. Rodríguez-Martínez, J. A.; Peterson-Kaufman, K. J.; Ansari, A. Z. Small-Molecule Regulators That Mimic Transcription Factors. *Biochim. Biophys. Acta* **2010**, *1799*, 768–774.
17. Xiao, X. S.; Yu, P.; Lim, H. S.; Sikder, D.; Kodadek, T. A Cell-Permeable Synthetic Transcription Factor Mimic. *Angew. Chem., Int. Ed.* **2007**, *46*, 2865–2868.
18. Kwon, Y.; Arndt, H.-D.; Mao, Q.; Choi, Y.; Kawazoe, Y.; Dervan, P. B.; Uesugi, M. Small Molecule Transcription Factor Mimic. *J. Am. Chem. Soc.* **2004**, *126*, 15940–15941.
19. Pandian, G. N.; Taniguchi, J.; Junetha, S.; Sato, S.; Han, L.; Saha, A.; AnandhaKumar, C.; Bando, T.; Nagase, H.; Vaijayanthi, T.; *et al*. Distinct DNA-Based Epigenetic Switches Trigger Transcriptional Activation of Silent Genes in Human Dermal Fibroblasts. *Sci. Rep.* **2014**, 4.
20. Pandian, G. N.; Nakano, Y.; Sato, S.; Morinaga, H.; Bando, T.; Nagase, H.; Sugiyama, H. A Synthetic Small Molecule for Rapid Induction of Multiple Pluripotency Genes in Mouse Embryonic Fibroblasts. *Sci. Rep.* **2012**, 2.
21. Dervan, P. B.; Edelson, B. S. Recognition of the DNA Minor Groove by Pyrrole-Imidazole Polyamides. *Curr. Opin. Struct. Biol.* **2003**, *13*, 284–299.
22. Gottesfeld, J. M.; Neely, L.; Trauger, J. W.; Baird, E. E.; Dervan, P. B. Regulation of Gene Expression by Small Molecules. *Nature* **1997**, *387*, 202–205.
23. Melander, C.; Burnett, R.; Gottesfeld, J. M. Regulation of Gene Expression with Pyrrole–Imidazole Polyamides. *J. Biotechnol.* **2004**, *112*, 195–220.
24. Nyanguile, O.; Uesugi, M.; Austin, D. J.; Verdine, G. L. A Nonnatural Transcriptional Coactivator. *Proc. Natl. Acad. Sci. U.S.A.* **1997**, *94*, 13402–13406.
25. Murakami, K.; Elmlund, H.; Kalisman, N.; Bushnell, D. A.; Adams, C. M.; Azubel, M.; Elmlund, D.; Levi-Kalisman, Y.; Liu, X.; Gibbons, B. J.; *et al*. Architecture of an RNA Polymerase II Transcription Pre-Initiation Complex. *Science* **2013**, 342.
26. Cantin, G. T.; Stevens, J. L.; Berk, A. J. Activation Domain–Mediator Interactions Promote Transcription Preinitiation Complex Assembly on Promoter DNA. *Proc. Natl. Acad. Sci. U.S.A.* **2003**, *100*, 12003–12008.
27. Hodel, M. R.; Corbett, A. H.; Hodel, A. E. Dissection of a Nuclear Localization Signal. *J. Biol. Chem.* **2001**, *276*, 1317–1325.
28. Tkachenko, A. G.; Xie, H.; Coleman, D.; Glomm, W.; Ryan, J.; Anderson, M. F.; Franzen, S.; Feldheim, D. L. Multifunctional Gold Nanoparticle–Peptide Complexes for Nuclear Targeting. *J. Am. Chem. Soc.* **2003**, *125*, 4700–4701.
29. Krpetić, Ž.; Saleemi, S.; Prior, I. A.; Sée, V.; Qureshi, R.; Brust, M. Negotiation of Intracellular Membrane Barriers by TAT-Modified Gold Nanoparticles. *ACS Nano* **2011**, *5*, 5195–5201.
30. Krpetić, Ž.; Singh, I.; Su, W.; Guerrini, L.; Faulds, K.; Burley, G. A.; Graham, D. Directed Assembly of DNA-Functionalized Gold Nanoparticles Using Pyrrole–Imidazole Polyamides. *J. Am. Chem. Soc.* **2012**, *134*, 8356–8359.
31. Lee, C. W.; Arai, M.; Martinez-Yamout, M. A.; Dyson, H. J.; Wright, P. E. Mapping the Interactions of the p53 Transactivation Domain with the KIX Domain of CBP. *Biochemistry* **2009**, *48*, 2115–2124.
32. Akey, C. W.; Radermacher, M. Architecture of the Xenopus Nuclear Pore Complex Revealed by Three-Dimensional Cryo-electron Microscopy. *J. Cell Biol.* **1993**, *122*, 1–19.
33. Hoelz, A.; Debler, E. W.; Blobel, G. The Structure of the Nuclear Pore Complex. *Annu. Rev. Biochem.* **2011**, *80*, 613–643.
34. Grossman, E.; Medalia, O.; Zwerger, M. Functional Architecture of the Nuclear Pore Complex. *Ann. Rev. Biophys.* **2012**, *41*, 557–584.
35. Karlić, R.; Chung, H.-R.; Lasserre, J.; Vlahoviček, K.; Vingron, M. Histone Modification Levels Are Predictive for Gene Expression. *Proc. Natl. Acad. Sci. U.S.A.* **2010**, *107*, 2926–2931.
36. Pang, Z. P.; Yang, N.; Vierbuchen, T.; Ostermeier, A.; Fuentes, D. R.; Yang, T. Q.; Citri, A.; Sebastiano, V.; Marro, S.; Sudhof, T. C.; *et al*. Induction of Human Neuronal Cells by Defined Transcription Factors. *Nature* **2011**, *476*, 220–223.
37. Takahashi, K.; Yamanaka, S. Induction of Pluripotent Stem Cells from Mouse Embryonic and Adult Fibroblast Cultures by Defined Factors. *Cell* **2006**, *126*, 663–676.
38. Hou, P.; Li, Y.; Zhang, X.; Liu, C.; Guan, J.; Li, H.; Zhao, T.; Ye, J.; Yang, W.; Liu, K.; *et al*. Pluripotent Stem Cells Induced from Mouse Somatic Cells by Small-Molecule Compounds. *Science* **2013**, *341*, 651–654.
39. Jung, J.; Solanki, A.; Memoli, K. A.; Kamei, K.-i.; Kim, H.; Drahl, M. A.; Williams, L. J.; Tseng, H.-R.; Lee, K. Selective Inhibition of Human Brain Tumor Cells through Multifunctional Quantum-Dot-Based siRNA Delivery. *Angew. Chem., Int. Ed.* **2010**, *49*, 103–107.

40. Shah, S.; Solanki, A.; Sasmal, P. K.; Lee, K.-B. Single Vehicular Delivery of siRNA and Small Molecules to Control Stem Cell Differentiation. *J. Am. Chem. Soc.* **2013**, *135*, 15682–15685.
41. Ferreira, L.; Karp, J. M.; Nobre, L.; Langer, R. New Opportunities: The Use of Nanotechnologies to Manipulate and Track Stem Cells. *Cell Stem Sell* **2008**, *3*, 136–146.
42. Solanki, A.; Chueng, S.-T. D.; Yin, P. T.; Kappera, R.; Chhowalla, M.; Lee, K.-B. Axonal Alignment and Enhanced Neuronal Differentiation of Neural Stem Cells on Graphene-Nanoparticle Hybrid Structures. *Adv. Mater.* **2013**, *25*, 5477–5482.
43. Shah, B.; Yin, P. T.; Ghoshal, S.; Lee, K.-B. Multimodal Magnetic Core−Shell Nanoparticles for Effective Stem-Cell Differentiation and Imaging. *Angew. Chem., Int. Ed.* **2013**, *52*, 6190–6195.
44. Solanki, A.; Shah, S.; Memoli, K. A.; Park, S. Y.; Hong, S.; Lee, K.-B. Controlling Differentiation of Neural Stem Cells Using Extracellular Matrix Protein Patterns. *Small* **2010**, *6*, 2509–2513.
45. Biel, M.; Wascholowski, V.; Giannis, A. Epigenetics—An Epicenter of Gene Regulation: Histones and Histone-Modifying Enzymes. *Angew. Chem., Int. Ed.* **2005**, *44*, 3186–3216.
46. Koren, E.; Torchilin, V. P. Cell-Penetrating Peptides: Breaking through to the Other Side. *Trends Mol. Med.* **2012**, *18*, 385–393.
47. Kurreck, J. RNA Interference: From Basic Research to Therapeutic Applications. *Angew. Chem., Int. Ed.* **2009**, *48*, 1378–1398.
48. Haase, M.; Schäfer, H. Upconverting Nanoparticles. *Angew. Chem., Int. Ed.* **2011**, *50*, 5808–5829.